TRIM32 – a putative regulator of NDP52 mediated selective autophagy

Katrine Stange Overå, Zambarlal Bhujabal, Juncal Garcia Garcia, Eva Sjøttem*

Molecular Cancer Research Group, Department of Medical Biology, University of Tromsø – The Arctic University of Norway, 9037 Tromsø, Norway

*Corresponding author. Tel: +47 776 46425; E-mail: eva.sjottem@uit.no

Running title: TRIM32 regulates NDP52 activity?

Keywords: TRIM32, NDP52, Mitophagy, ULK1, Ubiquitylation

ABSTRACT

Several members of the tripartite motif (TRIM) family proteins are identified as regulators of autophagy. They associate with autophagy factors and serve as platforms for recruitment of activated ULK1 and BECLIN1, promoting phagophore formation and expansion. Recently, TRIM32 was identified as an activator of ULK1 in atrophic muscle cells. Mutations in the C-terminal NHL domains of TRIM32 is linked to Limb-Girdle-Muscular-Dystrophy 2H, while a mutation in its BBox causes Bardet-Biedl-syndrome type 11. Here we show that TRIM32 affects the protein levels of the sequestosome-like-receptors (SLRs) implicated in selective autophagy. Conversely, TRIM32 is directed to autophagic degradation by the SLRs. The cargo receptor NDP52 is important for recruiting ULK1 and the autophagic machinery to damaged mitochondria. Our data show that TRIM32 mediates ubiquitylation of NDP52, and that mitophagy is impaired in TRIM32 KO cells compared to normal cells and TRIM32 KO cells reconstituted with TRIM32. Furthermore, introduction of E3 ligase active TRIM32 in the TRIM32 KO cells stabilises ULK1 and facilitates TBK1 autophosphorylation, while expression of the LGMD2H mutated version of TRIM32 do not. Collectively, this study identify TRIM32 as a potential regulator of NDP52, ULK1 and TBK1, facilitating mitophagy.

INTRODUCTION

Selective autophagy is a catabolic process that plays an important role in the maintenance of cellular homeostasis. It identifies and recycles unwanted or dysfunctional components, such as protein aggregates, damaged mitochondria, ferritin and intracellular pathogens (Rogov et al., 2014). In this way, selective autophagy protects from diseases such as cancer, neurodegeneration, and uncontrolled infections (Levine and Kroemer, 2019). Recent studies have revealed that selective autophagy is induced by cargo receptors that bind to their substrates and orchestrate the autophagy machinery to initiate phagophore assembly (Turco et al., 2019; Vargas et al., 2019). The most extensive studied cargo receptors are the family of sequestosome-like-receptors (SLRs); sequestosome-1 (p62/SQSTM1), nuclear dot protein 52 kDa (NDP52); neighbor of BRCA1 gene 1 (NBR1); Optineurin and Tax1-binding protein 1 (Tax1BP1) (Johansen and Lamark, 2011; Rogov et al., 2014). The SLRs seem to have at least partly overlapping functions, in which they recognize ubiquitylated cargo via their ubiquitin binding domains, oligomerize and interacts directly with the autophagy machinery via FIP200 and the ATG8s (Khaminets et al., 2016; Turco et al., 2019).

One of the main cargo receptors of damaged mitochondria is NDP52, which is recruited to depolarized mitochondria by the ubiquitin ligase PINK1 (Lazarou et al., 2015). Tethering of NDP52 to the mitochondria leads to positioning of the autophagy initiation complex including FIP200 and ULK1 on the mitochondria (Vargas et al., 2019). The process is facilitated by TBK1, and leads to activation of ULK1 and induction of mitophagy. A similar scenario takes place upon cellular infection of cytosol-invading bacteria (Ravenhill et al., 2019). Here, NDP52 recognizes Galectin-8 on the damaged bacterial-containing vacuole. This leads to recruitment of ULK1 and TBK1 via the ULK1 complex subunit FIP200 and the TBK1 adaptor SINTBAD, which promotes phagophore formation and xenophagy

Several members of the tripartite motif (TRIM) protein family of E3 ligases function as regulatory autophagy receptors, acting in precision autophagy (Kimura et al., 2015). They recruit the autophagy initiation complexes ULK1 and PI3Kc1 to their substrates to facilitate autophagic degradation (Mandell et al., 2014). TRIM proteins are characterized by a RING-domain which constitutes the E3 ligase activity, one or two BBox domains, a coiled-coil domain and a variable C-terminal region (Reymond et al., 2001). The C-terminal domain of TRIM32 encompasses six NHL-repeats which are involved in dimerization and cargo recognition (Koliopoulos et al., 2016). Genetic mutations in the NHL domains cause the muscle disorder Limb Girdle Muscular Dystrophy 2H (LGMD2H), and is associated with impaired auto-

oligomerization and self-ubiquitination, and reduced TRIM32 expression level (Locke et al., 2009; Zhao et al., 2019). A missense-mutation in the BBox domain results in the disease Bardet-Biedl syndrome 11 (BBS11) which has a pleiotropic phenotype (Chiang et al., 2006). A recent study demonstrates that TRIM32 activates ULK1 and thereby facilitates autophagy in muscle cells upon atrophy induction (Di Rienzo et al., 2019). TRIM32 was linked to ULK1 via the autophagy cofactor AMBRA1. Importantly, the LGMD2H disease mutant of TRIM32 was unable to associate with ULK1 and induce autophagy. In another study, we show that TRIM32 mediates ubiquitylation of p62/SQSTM1, leading to enhanced p62/SQSTM1 sequestration and degradation.

Here we show that TRIM32 downregulates the protein levels of all SLR proteins, without affecting their expression at the RNA level. Conversely, autophagic degradation of TRIM32 is dependent on the SLRs, and beside p62/SQSTM1 both NDP52 and NBR1 are able to direct TRIM32 to degradation in the lysosome. We reveal that TRIM32 interacts directly with and ubiquitylates NDP52. Furthermore, mitophagy induced by co-overexpression of FKBP8 and LC3A is significantly reduced in TRIM32 KO cells compared to normal HEK293 cells. Reintroduction of myc-TRIM32 into the KO cells restored the mitophagy activity. In line with this, TRIM32 enhances ULK1 stability and TBK1 autophosphorylation, both shown to facilitate NDP52 mediated mitophagy.

MATERIALS AND METHODS

Antibodies and reagents

The following primary antibodies were used: rabbit polyclonal antibody for TRIM32 (Proteintech, 10326-1-AP); rabbit polyclonal anti-GFP (Abcam, ab290); mouse monoclonal Myc-Tag (9B11) (Cell Signalling, #2276); rabbit polyclonal anti-LC3B (Sigma, L7543); rabbit polyclonal anti-Actin (Sigma, A2066); mouse monoclonal anti-p62 lck ligand (BD Biosciences, 610833); rabbit polyclonal anti-CALCOCO2/NDP52 (Sigma, HPA023195); rabbit polyclonal anti-TAX1BP1 (Sigma, HPA024432); mouse monoclonal mono- and polyubiquitinylated conjugates FK2 (Enzo, BML-PW8810); rabbit monoclonal anti-ULK1 (D8H5) (Cell Signalling, #8054); rabbit polyclonal anti-GABARAP (MBL, PM037); rabbit monoclonal anti-TBK1 (Millipore, 108A429); rabbit monoclonal anti-Phsopho-TBK1/NAK (Cell Signalling, #5483); mouse monoclonal anti-NBR1 (Santa Cruz, sc-130380). The following secondary antibodies were used: Horseradish-peroxidase (HRP)-conjugated goat anti-rabbit IgG (BD

Biosciences, 554021); HRP-conjugated goat anti-mouse Ig (BD Biosciences, 554002); HRP-conjugated anti-Biotin antibody (Cell Signalling, #7075); IRDye 800CW Goat anti-Rabbit IgG (Li-Cor, 925-32211); IRDye 680RD Goat anti-Mouse IgG (Li-Cor, 925-68070). The following fluorescent secondary antibodies were used: Alexa Fluor® 488-conjugated goat anti-mouse IgG (Life Technologies, A-11029); Alexa Fluor® 555-conjugated goat anti-rabbit IgG (Life Technologies, A-11008). The reagents used were Hanks Balanced salt solution (Sigma, H8264).

Plasmids

Plasmids used in this study are listed in Table 1.

Table 1: Plasmids used in this study

pDest Myc	(Lamark et al., 2003)
pDest Myc TRIM32	(Overå et al., 2019)
pDest Myc TRIM32 D487N	(Overå et al., 2019)
pDest Myc TRIM32 P130S	(Overå et al., 2019)
pDest Myc NDP52	(Abudu et al., 2019)
pDest mCherry-YFP TRIM32	(Overå et al., 2019)
pDest EGFP-C1	(Lamark et al., 2003)
pDest EGFP TRIM32	(Overå et al., 2019)
pDest EGFP TRIM32 D487N	(Overå et al., 2019)
pDest EGFP TRIM32 P130S	(Overå et al., 2019)
pDest EGFP ULK1	(Alemu et al., 2012)
pDest Myc FKBP8	(Bhujabal et al., 2017)
mCherry-EGFP-OMP25-TM	(Wang et al., 2015)
pDest-3XFlag-LC3A	(Bhujabal et al., 2017)

Cell culture and transfections

HeLa (ATCC, CCL2), HEK293 (ATCC, CRL-1573), HEK293 FlpIn T-Rex (ThermoFisher, R714-07), HEK293 FlpIn TRIM32 KO (Overå et al., 2019); HEK293 FlpIn TRIM32 KO myc-TRIM32^{WT} (Overå et al., 2019) , HEK293 FlpIn TRIM32 KO myc-TRIM32^{P130S} (Overå et al., 2019), HEK293 FlpIn TRIM32 KO myc-TRIM32^{D487N} (Overå et al., 2019), HeLa Penta KO (Lazarou et al., 2015), HeLa Penta KO EGFP NDP52 and HeLa Penta KO EGFP NBR1 cells were cultured in Dulbecco's modified eagle's medium (DMEM) (Sigma, D6046) with 10% fetal bovine serum and 1% streptomycin-penicillin (Sigma, P4333). Sub-confluent cells were

transfected using TransIT-LT1 (Mirus, MIR2300) or Metafectene Pro (Biontex, T040) following the manufacturer's instructions.

Recombinant protein production and GST pulldown analysis

GST or GST-tagged proteins were expressed in *Escherichia coli* strain SoluBL21 (Genlantis, #C700200). Protein expression was induced by treating overnight bacterial culture with 50µg/ml Isopropyl β-D-1-thiogalactopyranoside (IPTG). GST or GST fusion proteins were purified and immobilized on Glutathione-Sepharose 4 Fast Flow beads (GE Healtcare, 17-5132-01). Myc-tagged proteins were *in vitro* translated using the TNT T7 reticulocyte Lysate system (Promega, #14610) in the presence of ^{35}S-methionine. *In vitro* translated protein or total cell lysate was pre-incubated with 10µl glutathione sepharose beads and 100µl of NETN buffer (50mM Tris pH 8.0; 150mM NaCl; 1 mM EDTA; 0.5% Nonidet P-40) with cOmplete Mini EDTA-free protease inhibitor mixture tablets (1 tablet/10ml) (Roche Applied Science, 11836170001) for 1hr at 4°C to reduce unspecific binding. Pre-incubated lysate was then incubated with the immobilized GST fusion protein for 2hrs at 4°C. Beads were washed five times with NETN buffer, boiled with 2xSDS gel loading buffer (125mM Tris pH 7.5; 4% SDS; 0.04% bromphenol blue; 8% sucrose; 100mM dithiolthreitol) and subjected to SDS-PAGE. Gels were stained with Coomassie Brilliant Blue R-250 Dye (Thermofisher scientific, #20278) to visualize GST fusion proteins and then vacuum-dried. Signals from ^{35}S-labelled proteins were detected by a Fujifilm bioimaging analyzer BAS-5000 (Fujifilm).

Western Blotting

Cells were seeded in 6 well dishes and treated as indicated. Cells were lysed in 1xSDS buffer (50mM Tris pH 7.4; 2% SDS; 10% Glycerol) supplemented with 200mM dithiothreitol (DTT, Sigma, #D0632) and heated at 100°C for 10 minutes. Protein concentration was measured using the Pierce BCA Protein Assay Kit (Thermofisher Scientific, #23227). Equal amounts of protein were resolved by SDS-PAGE and transferred to nitrocellulose membrane (Sigma, GE10600003). The membrane was stained with Ponceau S (Sigma, P3504), blocked with 5% non-fat dry milk in 1% TBS-T (0.2M Tris pH 8; 1.5M NaCl and 0.05% Tween20 (Sigma, P9416)) and then incubated with indicated primary antibodies for 24h. The membrane was washed three times for 10 minutes each with TBS-T followed by incubation with secondary antibody for 1h. The membrane was washed three times for 10 minutes and analyzed by enhanced chemiluminescence using the ImageQuant LAS 4000 (GE Lifescience).

Ubiquitination Assay

Subconfluent HEK293 FlpIn TRIM32 KO cells seeded in 6-well dishes were transiently co-transfected with pDEST myc-NDP52 (500 ng) and pDEST EGFP-TRIM32^{WT} (500 ng), pDEST EGFP-TRIM32^{P130S}(500 ng), or pDEST EGFP-TRIM32^{D487N}(500 ng) using Metafecten Pro (Biontex, T040). Subconfluent TRIM32 KO cells and reconstituted TRIM32 KO with Myc-TRIM32 WT, Myc-TRIM32 P130S or Myc-TRIM32 D487N cells were transfected with pDEST EGFP-ULK1 (500 ng) using Metafectene Pro. One day post transfection, the cells were lysed in modified Radioimmunoprecipitation assay (RIPA) buffer (50mM Tris pH 7.5; 150mM NaCl; 1mM EDTA; 1% NP40; 0.25% Triton-X-100) supplemented with cOmplete Mini EDTA-free protease inhibitor cocktail tablets (Roche, #11836170001) and phosphatase inhibitor cocktail (Merck Millipore, #524625) by shaking at 4°C for 30 min. The cell lysate was centrifuged at 10.000 x g for 10 min. The resulting supernatant was incubated with Myc-TRAP (Chromotek, yta-20) or GFP-TRAP (Chromotek, gta-20). They were washed five times in RIPA buffer before boiling in 2X SDS gel loading buffer. This was followed by protein identification by immunoblotting as previously described but on Immobilon-FL PVDF membrane (Millipore, IPFL00010), blocked with Odyssey® blocking buffer (PBS) (LI-COR Biosciences, #927-40000) and scanned on Odyssey CLx Imager (LI-COR).

Immunostaining and Fluorescence confocal microscopy

Subconfluent cells were grown on coverslips (VWR, #631-0150) coated with Fibronectin (Sigma, F1141) and treated as indicated. They were fixed in 4% formaldehyde for 20min at R.T., permeabilized with methanol at RT for 5min, blocked in 5% goat serum/PBS or 5%BSA/PBS and incubated at room temperature with a specific primary antibody followed by Alexa Fluor 488 or 555 conjugated secondary antibody and DAPI. Confocal images were obtained using a 63x/NA1.4 oil immersion objective on an LSM780 system or LSM800 system and the ZEN software (Zeiss). Quantification of cells containing red only dots in the mCherry-EYFP-double tag assay was done manually in three independent experiments.

RT-PCR/QPCR

Total RNA was extracted from HEK 293T FlpIn cells TRIM32 KO cells reconstituted with TRIM32 WT, TRIM32 P130S mutant and TRIM32 D487N mutant using the Gene Elute Mammalian Total RNA Miniprep kit (Sigma). The RNA quality was checked by 260/280 nm absorption using a NanoDrop 2000 spectrophotometer (Thermo Fisher scientific). First-strand cDNA was prepared using the High Capacity RNA-to-cDNA Kit according to the

manufacturer's instruction. Amplification was performed with SYBR green kit FastStart Essential DNA Green Master (Roche) in a 20 µl reaction. Reactions were run with the following cycling parameters temperatures (58 degrees aneling temperature for Actin, GAPDH, NDP52 and Optineurin and 60 for p62 and NBR1) and 45 cycles by Lightcycler 96 (Roche). All reactions were performed in triplicate. Relative expression levels were calculated after correction for the expression of Actin and GAPDH as an endogenous reference. The primer sequences used for p62 fw and reverse were 5'-ggagaagagcagctcacagcca-3' and 5'-ccttcagccctgtgggtccct-3', NBR1 forward and reverse 5'-ggaagcagaagaagacctgagtg-3' and 5'-ccagagtctgtgaggtcgtgag-3', and NDP52 fw and reverse 5'-accatggaggagaccatcaa-3' and 5'-ttctggacggaattggaaag-3', and standards (Actin and GAPDH) fw and reverse Actin 5'-tgacggtcaggtcatcactatcggcaatga-3' and 5'-ttgatcttcatggtgataggagcgagggca-3', gapdh 5'-ggcactgtcaaggctgaaaacg-3' and 5'-ggagatgagatgataccacgcttag-3'.

Mitophagy assay

HEK293 FlpIn T-Rex cells, TRIM32 KO cells and TRIM32 KO cells reconstituted with Myc-TRIM32 were seeded on fibronectin-coated coverslips two days before transient co-transfection with the plasmids mCherry-EGFP-OMP25-TM (100 ng), pDEST-3xFlag-LC3A (100 ng) and pDEST-myc-FKBP8 (100 ng) using the Trans-IT (Mirus) transfection reagent. One day post transfection, the cells were fixated in 4% Formaldehyde, 15 minutes at R.T., stained with DAPI (5 min). The cells were imaged using a Zeiss800 confocal microscope, and z-stack images of at least 100 cells per condition per experiment were manually quantitated for RedOnly stuctures using the ZEN software (Zeiss).

Statistics

All experiments were repeated at least three times, unless otherwise specified. Error bars represent the standard deviation, or standard error of the mean as indicated in the Figure legends. Two-sided unpaired, homoscedastic Student T-Tests, were performed to assess significant differences between populations. Replicates were not pooled for statistical analyses.

RESULTS AND DISCUSSION

In a previous report we showed that TRIM32 is an autophagy substrate. Its lysosomal degradation was mediated by selective autophagy, dependent on ATG7 and the sequestosome-like receptors (SLRs). Reintroduction of p62/SQSTM1 in a cell line lacking the SLRs was

sufficient to direct autophagic degradation of TRIM32. However, knock out of p62/SQSTM1 did not abolish lysosomal degradation of TRIM32, suggesting that other SLRs may direct TRIM32 to autophagic degradation. Furthermore, we identified TRIM32 as an activator of p62/SQSTM1, facilitation p62/SQSTM1 sequestration and degradation. Here we set out to identify the importance of TRIM32 on SLR protein levels in HEK293 cells. Cell extracts from two different TRIM32 knock-out clones, KO#1 and KO#2 (Overå et al., 2019), reconstituted with myc-TRIM32 wild type or the disease mutants TRIM32^{D487N} and TRIM32^{P130S}, were exposed to antibodies against the SLRs p62/SQSTM1, NBR1, NDP52 and TAX1BP1 (Fig. 1A). Consistently, reintroduction of myc-TRIM32^{WT} or myc-TRIM32^{P130S} reduced the protein levels of the SLRs, suggesting enhanced SLR mediated selective autophagy (Fig. 1A,B). In contrast, reintroduction of the LGMD2H disease mutant form of TRIM32, TRIM32^{D487N}, did not affect the protein levels of the SLRs. As shown previously (Frosk et al., 2002)Overå et al., 2019), TRIM32^{WT} and TRIM32^{P130S} contain ubiquitylation activity and are themselves degraded by autophagy. TRIM32^{D487N} is not found to ubiquitylate itself or any target proteins, suggesting that mutations in the NHL-repeat region abolish its enzymatic activity and its ability to be degradation by autophagy. Western blot analyses of LC3B and Gabarap in the same cell extracts did not result in a reproducible change in their protein level or lipidation (Fig. 1A). This is in line with previous data showing that TRIM32 does not display any prominent effect on global autophagy, but instead on SLR mediated selective autophagy (Overå et al., 2019). In order to investigate whether the TRIM32 induced reduction of SLR expression was regulated at protein or RNA level, we analysed RNA expression by QPCR of representative SLRs in the same cell lines (Fig. 1C). Comparing SLR RNA levels in the reconstituted cell lines with the SLR RNA levels in the TRIM32 KO#1 cell line revealed no significant change in RNA expression. Together, our results show that catalytic active TRIM32 modify the protein levels of the SLRs. For p62/SQSTM1 we have shown that this is due to TRIM32 mediated ubiquitination of p62/SQSTM1 leading to enhanced p62/SQSTM1 autophagic activity. An interesting question to address is whether this is a general mechanism for all SLRs, pointing towards an important regulatory role of TRIM32 in selective autophagy.

We have previously shown that autophagic degradation of TRIM32 is strongly inhibited in a HeLa pentaKO cell line (Lazarou et al., 2015) lacking expression of the five SLRs (Overå et al., 2019). To identify if any of the SLRs beside p62/SQSTM1 were able to direct autophagic degradation of TRIM32, we established pentaKO cell lines stably expressing each of the SLRs. Transfection of mCherry-EYFP-tagged TRIM32 into these cell lines revealed that

reintroduction of NDP52 or NBR1 facilitated autophagic degradation of TRIM32 (Fig. 2). This suggests that each of the SLRs mediates autophagic degradation of TRIM32, and that they are independent of each other for facilitating this process.

The very consistent downregulation of NDP52 protein levels in the TRIM32 KO cells reconstituted with catalytic active TRIM32 (Fig. 1A), prompted us to investigate whether there is a direct interaction between TRIM32 and NDP52. GST-pulldown assays using immobilised GST-NDP52 or GST-p62/SQSTM1 expressed and purified from *E. coli* together with *in vitro* translated EGFP-TRIM32^{WT} or the disease mutants EGFP-TRIM32^{P130S} and EGFP-TRIM32^{D487N}, showed that there is a direct interaction between NDP52 and TRIM32 (Fig. 3A) *in vitro*. The interaction is weak, but stronger than the previously reported interaction between TRIM32 and p62/SQSTM1 (Fig. 1A). Both TRIM32^{WT} and the two disease mutants bound to NDP52, suggesting that the *in vitro* interaction is independent on the E3 ligase activity of TRIM32. Next, we applied immunofluorescence assays to determine if TRIM32 is colocalized with endogenous NDP52 in cells. TRIM32 KO cells, and TRIM32 KO cells reconstituted with myc-TRIM32^{WT} or the disease mutants myc-TRIM32^{P130S} and myc-TRIM32^{D487N}, were grown in normal medium or normal medium supplemented with the lysosomal inhibitor Bafilomycin A1, fixated and exposed to an NDP52 antibody (Fig. 3B). TRIM32^{WT} and both disease mutants colocalised with NDP52 in certain dots under normal conditions (Fig. 3B). Inhibition of the lysosome resulted in accumulation of larger NDP52 dots that colocalised with TRIM32^{WT} and TRIM32P^{130S}. However, the LGMD2H disease mutant TRIM32^{D487N}, which displays augmented E3 ligase activity and is not a substrate for autophagic degradation (Overå et al., 2019), did not accumulate in larger NDP52 dots upon BafA1 treatment. These results indicate that TRIM32, both WT and disease mutants, are enriched in certain NDP52 dots in cells under normal conditions. However, accumulation of TRIM32^{WT} and TRIM32^{P130S} but not TRIM32^{D487N} in NDP52 dots upon lysosomal inhibition, suggest that NDP52 mediated lysosomal degradation of TRIM32 is dependent on the E3 ligase activity of TRIM32. We therefore went on to test if NDP52 is a TRIM32 substrate. Immunoprecipitation of myc-NDP52 co-expressed with EGFP-TRIM32 WT and disease mutants in TRIM32 KO cells, revealed several slow-migrating myc-NDP52 forms in the cells expressing TRIM32^{WT} or TRIM32^{P130S}. In the precipitate from the TRIM32-D487N expressing cells, no such slow migrating NDP52 forms was observed (Fig. 3C). To identify if these slow-migrating NDP52 could represent mono and poly-ubiquitinated NDP52, the immonoprecipitates were blotted against an antibody recognising mono- and poly-ubiquitin (Fig. 3C, lower panels). Clearly, NDP52

immunoprecipitated from cells expressing the E3 ligase active forms of TRIM32, TRIM32^{WT} and TRIM32^{P130S}, is modified by ubiquitin. On the other hand, NDP52 precipitated from the cells expressing the E3 ligase inhibited form of TRIM32, TRIM32^{D487N}, is not recognised by the ubiquitin antibody. The upper panel in Figure 3C show that TRIM32^{WT} and TRIM32^{P130S} co-precipitate very well NDP52, while the association between TRIM32^{D487N} and NDP52 is weaker. Together, these data show that NDP52 interacts with TRIM32 *in vitro* and in cells, and that they colocalise in certain dots in cells. Furthermore, TRIM32 mediates ubiquitination of NDP52, and this ubiquitination seems to be important for NDP52 directed autophagic degradation of TRIM32.

Recent reports have demonstrated that NDP52 plays an important role in selective degradation of depolarized mitochondria (mitophagy) (Heo et al., 2015; Lazarou et al., 2015; Vargas et al., 2019). Tethering of NDP52 to the mitochondria recruited the ULK1 complex via FIP200 interactions, and the authors suggested that this recruitment initiated autophagosome biogenesis directly on the mitochondria (Vargas et al., 2019). Previously we found that TRIM32 mediated ubiquitylation of p62/SQSTM1 enhanced p62/SQSTM1 autophagic activity. In order to measure if TRIM32 could affect the autophagic activity of NDP52, we induced mitophagy in HEK293 FlpIn cells, and the TRIM32 KO and reconstituted cell line. Mitophagy induction was obtained by overexpression of FKBP8 and LC3A, and autophagic degradation of mitochondria measured using the double-tag mCherry-GFP-OMP25TM (Bhujabal et al., 2017) (Fig. 4A). In normal HEK293 cells, co-overexpression of FKBP8 and LC3A induced mitophagy in 10-12% of the cells (Fig. 4B). However, when TRIM32 was knocked out, the amount of cells undergoing mitophagy by FKBP8 and LC3A overexpression was reduced to 5%. Importantly, reintroduction of myc-TRIM32 in the TRIM32 KO cells restored the mitophagy activity (Fig. 4B). NDP52 is shown to recruit the ULK1 complex to the autophagy cargo, and thereby initiate mitophagy and xenophagy (Ravenhill et al., 2019; Vargas et al., 2019), and TRIM proteins are reported to control autophagy by modulating the activity of BECLIN1 and ULK1 (Mandell et al., 2014). Moreover, in atrophic muscle cells TRIM32 mediates induction of autophagy via ULK1 activation. This activation of ULK1 requires TRIM32 E3 ligase activity, and is impaired in atrophic muscle cells expressing the LGMD2H disease mutant TRIM32^{D487N} (Di Rienzo et al., 2019). Interestingly, Western Blot analyses of ULK1 expression levels in the TRIM32 KO cells, and TRIM32 KO cells reconstituted with myc-TRIM32^{WT}, myc-TRIM32^{P130S} or myc-TRIM32^{D487N}, revealed that ULK1 is strongly stabilised in the cells expressing myc-TRIM32^{WT} and myc-TRIM32^{P130S} (Fig. 4C). In contrast,

reintroduction of the LGMD2H disease mutant TRIM32^{D487N}, did not affect ULK1 protein levels (Fig. 4 C,D). K63-linked ubiquitination of ULK1 stimulates its kinase activity (Nazio et al., 2013). To assess if TRIM32 mediated stabilization of ULK1 is due to ubiquitination of ULK1, we immunoprecipitated ULK1 from HEK293 cells co-expressing TRIM32^{WT} or disease mutants with EGFP-ULK1. However, no increased ubiquitination of ULK1 could be detected (Fig. 4E). This is in line with the work of Di Rienzo et al. (2019), where they found that ULK1 is not a direct substrate of TRIM32 in their system. Instead, they showed that ULK1 associated with unanchored K63-linked polyubiquitin chains synthesized by TRIM32 in an AMBRA1 dependent manner, and this binding to polyubiquitin chains stimulated ULK1 activity, monitored as increased phosphorylation of VPS34(S249) and BECLIN1 (S15). TBK1 facilitates the association of NDP52 with the ULK1 complex on mitochondria leading to mitophagy, while a kinase-dead TBK1 does not (Vargas et al., 2019). Recruiting TBK1 to the mitochondria induced TBK1 S172 autophosphorylation. Furthermore, selective autophagy of cytosol-invading bacteria involves NDP52 meditated recruitment of the TBK1-SINTBAD and ULK1-FIP200 complexes to the bacteria containing vacuole, promoting phagophore formation (Ravenhill et al., 2019). Assessing the TBK1 S172 phosphorylation in the TRIM32 KO and reconstituted cell lines, revealed that the amount of S172 phosphorylated TBK1 is highly upregulated in the cells reconstituted with TRIM32 compared to the TRIM32 KO cells (Fig. 4F). Since TBK1 undergoes autophosphorylation at S172 when TBK1 is enriched at subcellular structures, this suggests that TRIM32 facilitates TBK1 recruitment and activation which is important for efficient mitophagy and xenophagy.

To sum up, here we show that TRIM32 affect the protein expression levels of the SLRs, while the SLRs on the other hand have the ability to direct TRIM32 for autophagic degradation. Focusing on cargo receptor NDP52, we reveal that TRIM32 interacts with NDP52 and subject it for ubiquitination. NDP52 is an important receptor for mitophagy, and in congruence we find that mitophagy is downregulated in the TRIM32 KO cells compared to normal HEK293 cells and the TRIM32 KO cells reconstituted with TRIM32. Furthermore, ULK1 is stabilised and TBK1 autophosphorylation upregulated in cells expressing active TRIM32 (Fig. 4G), but not in cells expressing the LGMD2H disease version of TRIM32 shown to have impaired E3 ligase activity. An important question to address in future study is whether the TRIM32 mediated ubiquitylation of NDP52 directly facilitates its role as a receptor in selective autophagy.

FIGURE LEGENDS

Figure 1: E3 ligase active TRIM32 downregulates the protein levels of the sequestosome-like cargo receptors. A) Western blot showing the protein levels of the autophagy cargo receptors p62/SQSTM1, NBR1, NDP52 and TAX1BP1, and the autophagy marker proteins LC3B and GABARAP, in TRIM32 KO cells, and TRIM32 KO cells reconstituted with stable expression of myc-TRIM32^{WT}, myc-TRIM32^{P130S}, and myc-TRIM32^{D487N}. Actin serves as loading control, and the blot against TRIM32 shows the expression levels of the various TRIM32 proteins in the reconstituted cells. A biotinylated molecular weight marker is shown to the right. **B)** Quantitation of the band intensities from three Western blots as represented in A. The bar graphs represent the average band intensities normalized to the corresponding actin band from three independent experiments with s.e.m. The band intensities were quantitated by the use of ImageJ. **C)** RNA levels of the SLRs p62/SQSTM1, NBR1 and NDP52 in the reconstituted TRIM32^{WT}, TRIM32^{P130S} and TRIM32^{D487N} expressing cell lines relative to the RNA levels in the TRIM32 KO cell line. The graphs represent the average relative RNA levels with s.e.m. obtained by QPCR in three independent experiments, each performed in triplicate.

Figure 2: The cargco receptors NDP52 and NBR1 direct TRIM32 to autophagic degradation. A) Normal HeLa cells and cells that were genetically knocked out for the 5 SLRs (pentaKO), or pentaKO cells reconstituted with stable expression of EGFP-NDP52 or EGFP-NBR1 as indicated to the right, were transfected with mCherry-EYFP-TRIM32 expression plasmids. One day post transfection the cells were fixated, stained with DAPI and imaged using a Zeiss780 confocal microscope. Scale bar (10 μm). **B)** Quantitation of the number of yellow dots and red-only dots in the cells transfected as described in A. The graphs display the average number of yellow and RedOnly dots with S.D. in cells with mCherry-EYFP-TRIM32 dots, obtained in three independent experiments.

Figure 3: TRIM32 associates with and ubiquitylates NDP52. A) GST-pulldown assays using ^{35}S-labeled Myc-TRIM32, Myc-TRIM32^{P130S}, or Myc-TRIM32^{D487N} and recombinant GST, GST-p62 and GST-NDP52 immobilized on Glutathione Sepharose beads. Quantifications of the binding of wild type and mutant constructs to the GST proteins are presented as percentage binding relative to the 5% input. The bars represent the average band intensities with s.d. quantitated using ImageJ, of three independent experiments. **B)** Representative images of

HEK293 FlpIn TRIM32 KO cells, and the TRIM32 KO cells reconstituted with myc-TRIM32^{WT}, myc-TRIM32^{P130S} or myc-TRIM32^{D487N} cells in full media or starved with HBSS (2 hrs) fixed and stained with antibodies for NDP52. Images were obtained using a ZEISS780 confocal laser scanning microscope, and the co-localization monitored using the ZEN software**.** Scale bar (10 μm). **C)** Myc-NDP52 expression plasmid was cotransfected with EGFP-TRIM32, EGFP-TRIM32^{P130S} or EGFP-TRIM32^{D487N} expression constructs in the HEK293 TRIM32 KO cell line. Myc-NDP52 was immunoprecipitated using a myc-trap and precipitated NDP52 detected using an anti-myc antibody. The EGFP-TRIM proteins were detected using an anti-GFP antibody, and ubiquitin by using an FK2 antibody recognizing both mono-and poly-ubiquitin chains. * indicates ubiquitylated NDP52.

Figure 4: TRIM32 stabilises ULK1 and facilitates TBK1 phosphorylation and mitophagy. **A)** HEK293 FlpIn cells, HEK293 TRIM32 KO cells, or HEK293 TRIM32 KO cells reconstituted with myc-TRIM32 were transiently transfected with expression plasmids for the mitochondria marker mCherry-GFP-OMP25-TM, 3xFlag LC3A and mitophagy receptor myc-FKBP8. The appearance of RedOnly structures indicates acidified mitochondria. **B)** Quantitation of the cells representated in A displaying RedOnly dots indicative of mitophagy activity. The bars represent the average with s.e.m. of three independent experiments, each including > 100 cells per condition. **C)** Western blot showing the protein levels of ULK1 in TRIM32 KO cells, and TRIM32 KO cells reconstituted with stable expression of myc-TRIM32^{WT}, myc-TRIM32^{P130S}, and myc-TRIM32^{D487N}. Actin serves as loading control, and the blot against TRIM32 shows the expression levels of the various TRIM32 proteins in the reconstituted cells. A biotinylated molecular weight marker is shown to the right. **D)** Quantitation of the band intensities from three Western blots as represented in C. The bar graphs represent the average band intensities normalized to the corresponding actin band from three independent experiments with s.e.m. The band intensities were quantitated by the use of ImageJ. **E)** EGFP-ULK1 expression plasmid was transfected into TRIM32KO cell lines reconstituted with myc-TRIM32, myc-TRIM32^{P130S} or myc-TRIM32^{D487N}. EGFP-ULK1 was immunoprecipitated using a GFP-trap and precipitated EGFP-ULK1 detected using an anti-GFP antibody. The myc-TRIM proteins were detected using an anti-myc antibody, and ubiquitin by using an FK2 antibody recognizing both mono-and poly-ubiquitin chains. **F)** Western blot showing the protein levels of phosphorylated TBK1 and TBK1 as indicated to the right, in TRIM32 KO cells, and TRIM32 KO cells reconstituted with stable expression of myc-

TRIM32^{WT}, myc-TRIM32^{P130S}, and myc-TRIM32^{D487N}. The extracts are from cells exposed to normal medium and cells starved in HBSS for two hours, as indicated above. The band intensities quantitated using ImageJ and correlated to actin, are displayed below. Actin serves as loading control, and the blot against TRIM32 shows the expression levels of the various TRIM32 proteins in the reconstituted cells. **G)** TRIM32 facilitates mitophagy, enhances TBK1 phosphorylation and ULK1 expression that are important for phagophore formation on the mitochondria, and induces ubiquitylation of NDP52.

ACKNOWLEDGEMENT

We thank Richard Youle, National Institutes of Health, Bethesda, MD 20892, USA, for the generous gift of the pentaKO cell line, and Yakubu P. Abudu, UiT – The Arctic University of Norway, for the gift of the EGFP-NDP52 and EGFP-NBR1 reconstituted pentaKO cell lines. Thanks to the Advanced Microscopy Core Facility at UiT – The Arctic University of Norway, for the use of instrumentation. This work was supported by PhD grants to K.S.O and J.G.G from UiT – The Arctic University of Norway, and by the Research Council of Norway (TOPPFORSK program grant #249884 to T.J),

REFERENCES

Abudu, Y.P., S. Pankiv, B.J. Mathai, T. Lamark, T. Johansen, and A. Simonsen. 2019. NIPSNAP1 and NIPSNAP2 act as "eat me" signals to allow sustained recruitment of autophagy receptors during mitophagy. *Autophagy*. 15:1845-1847.

Alemu, E.A., T. Lamark, K.M. Torgersen, A.B. Birgisdottir, K.B. Larsen, A. Jain, H. Olsvik, A. Overvatn, V. Kirkin, and T. Johansen. 2012. ATG8 family proteins act as scaffolds for assembly of the ULK complex: sequence requirements for LC3-interacting region (LIR) motifs. *J Biol Chem*. 287:39275-39290.

Bhujabal, Z., A.B. Birgisdottir, E. Sjottem, H.B. Brenne, A. Overvatn, S. Habisov, V. Kirkin, T. Lamark, and T. Johansen. 2017. FKBP8 recruits LC3A to mediate Parkin-independent mitophagy. *EMBO Rep*. 18:947-961.

Chiang, A.P., J.S. Beck, H.J. Yen, M.K. Tayeh, T.E. Scheetz, R.E. Swiderski, D.Y. Nishimura, T.A. Braun, K.Y. Kim, J. Huang, K. Elbedour, R. Carmi, D.C. Slusarski, T.L. Casavant, E.M. Stone, and V.C. Sheffield. 2006. Homozygosity mapping with SNP arrays identifies TRIM32, an E3 ubiquitin ligase, as a Bardet-Biedl syndrome gene (BBS11). *Proc Natl Acad Sci U S A*. 103:6287-6292.

Di Rienzo, M., M. Antonioli, C. Fusco, Y. Liu, M. Mari, I. Orhon, G. Refolo, F. Germani, M. Corazzari, A. Romagnoli, F. Ciccosanti, B. Mandriani, M.T. Pellico, R. De La Torre, H. Ding, M. Dentice, M. Neri, A. Ferlini, F. Reggiori, M. Kulesz-Martin, M. Piacentini, G. Merla, and G.M. Fimia. 2019. Autophagy induction in atrophic muscle cells requires ULK1 activation by TRIM32 through unanchored K63-linked polyubiquitin chains. *Sci Adv*. 5:eaau8857.

Frosk, P., T. Weiler, E. Nylen, T. Sudha, C.R. Greenberg, K. Morgan, T.M. Fujiwara, and K. Wrogemann. 2002. Limb-girdle muscular dystrophy type 2H associated with mutation in TRIM32, a putative E3-ubiquitin-ligase gene. *Am J Hum Genet*. 70:663-672.

Heo, J.M., A. Ordureau, J.A. Paulo, J. Rinehart, and J.W. Harper. 2015. The PINK1-PARKIN Mitochondrial Ubiquitylation Pathway Drives a Program of OPTN/NDP52 Recruitment and TBK1 Activation to Promote Mitophagy. *Mol Cell*. 60:7-20.

Johansen, T., and T. Lamark. 2011. Selective autophagy mediated by autophagic adapter proteins. *Autophagy*. 7:279-296.

Khaminets, A., C. Behl, and I. Dikic. 2016. Ubiquitin-Dependent And Independent Signals In Selective Autophagy. *Trends Cell Biol*. 26:6-16.

Kimura, T., A. Jain, S.W. Choi, M.A. Mandell, K. Schroder, T. Johansen, and V. Deretic. 2015. TRIM-mediated precision autophagy targets cytoplasmic regulators of innate immunity. *J Cell Biol*. 210:973-989.

Koliopoulos, M.G., D. Esposito, E. Christodoulou, I.A. Taylor, and K. Rittinger. 2016. Functional role of TRIM E3 ligase oligomerization and regulation of catalytic activity. *EMBO J*. 35:1204-1218.

Lamark, T., M. Perander, H. Outzen, K. Kristiansen, A. Overvatn, E. Michaelsen, G. Bjorkoy, and T. Johansen. 2003. Interaction codes within the family of mammalian Phox and Bem1p domain-containing proteins. *The Journal of biological chemistry*. 278:34568-34581.

Lazarou, M., D.A. Sliter, L.A. Kane, S.A. Sarraf, C. Wang, J.L. Burman, D.P. Sideris, A.I. Fogel, and R.J. Youle. 2015. The ubiquitin kinase PINK1 recruits autophagy receptors to induce mitophagy. *Nature*. 524:309-314.

Levine, B., and G. Kroemer. 2019. Biological Functions of Autophagy Genes: A Disease Perspective. *Cell*. 176:11-42.

Locke, M., C.L. Tinsley, M.A. Benson, and D.J. Blake. 2009. TRIM32 is an E3 ubiquitin ligase for dysbindin. *Hum Mol Genet*. 18:2344-2358.

Mandell, M.A., T. Kimura, A. Jain, T. Johansen, and V. Deretic. 2014. TRIM proteins regulate autophagy: TRIM5 is a selective autophagy receptor mediating HIV-1 restriction. *Autophagy*. 10:2387-2388.

Nazio, F., F. Strappazzon, M. Antonioli, P. Bielli, V. Cianfanelli, M. Bordi, C. Gretzmeier, J. Dengjel, M. Piacentini, G.M. Fimia, and F. Cecconi. 2013. mTOR inhibits autophagy by controlling ULK1 ubiquitylation, self-association and function through AMBRA1 and TRAF6. *Nat Cell Biol*. 15:406-416.

Overå, K., Garcia, J.G., Bhujabal, Z., Jain, A., Øvervatn, A., Larsen, K.B., Deretic, V., Johansen, T., Lamark, T., and Sjøttem, E. 2019. TRIM32, but not its muscular dystrophy-associated mutant, positively regulates and is targeted to autophagic degradation by p62/SQSTM. *J. Cell Science*. PMID 31828304.

Ravenhill, B.J., K.B. Boyle, N. von Muhlinen, C.J. Ellison, G.R. Masson, E.G. Otten, A. Foeglein, R. Williams, and F. Randow. 2019. The Cargo Receptor NDP52 Initiates Selective Autophagy by Recruiting the ULK Complex to Cytosol-Invading Bacteria. *Mol Cell*. 74:320-329 e326.

Reymond, A., G. Meroni, A. Fantozzi, G. Merla, S. Cairo, L. Luzi, D. Riganelli, E. Zanaria, S. Messali, S. Cainarca, A. Guffanti, S. Minucci, P.G. Pelicci, and A. Ballabio. 2001. The tripartite motif family identifies cell compartments. *EMBO J*. 20:2140-2151.

Rogov, V., V. Dotsch, T. Johansen, and V. Kirkin. 2014. Interactions between autophagy receptors and ubiquitin-like proteins form the molecular basis for selective autophagy. *Mol Cell*. 53:167-178.

Turco, E., D. Fracchiolla, and S. Martens. 2019. Recruitment and Activation of the ULK1/Atg1 Kinase Complex in Selective Autophagy. *J Mol Biol*.

Vargas, J.N.S., C. Wang, E. Bunker, L. Hao, D. Maric, G. Schiavo, F. Randow, and R.J. Youle. 2019. Spatiotemporal Control of ULK1 Activation by NDP52 and TBK1 during Selective Autophagy. *Mol Cell*. 74:347-362 e346.

Wang, Y., M. Serricchio, M. Jauregui, R. Shanbhag, T. Stoltz, C.T. Di Paolo, P.K. Kim, and G.A. McQuibban. 2015. Deubiquitinating enzymes regulate PARK2-mediated mitophagy. *Autophagy*. 11:595-606.

zhao, M., K. Song, W. Hao, L. Wang, G. Patil, Q. Li, L. Xu, F. Hua, B. Fu, J.C. Schwamborn, M.E. Dorf, and S. Li. 2019. Non-proteolytic ubiquitination of OTULIN regulates NF-kappaB signaling pathway. *Journal of molecular cell biology*.

Figure 1

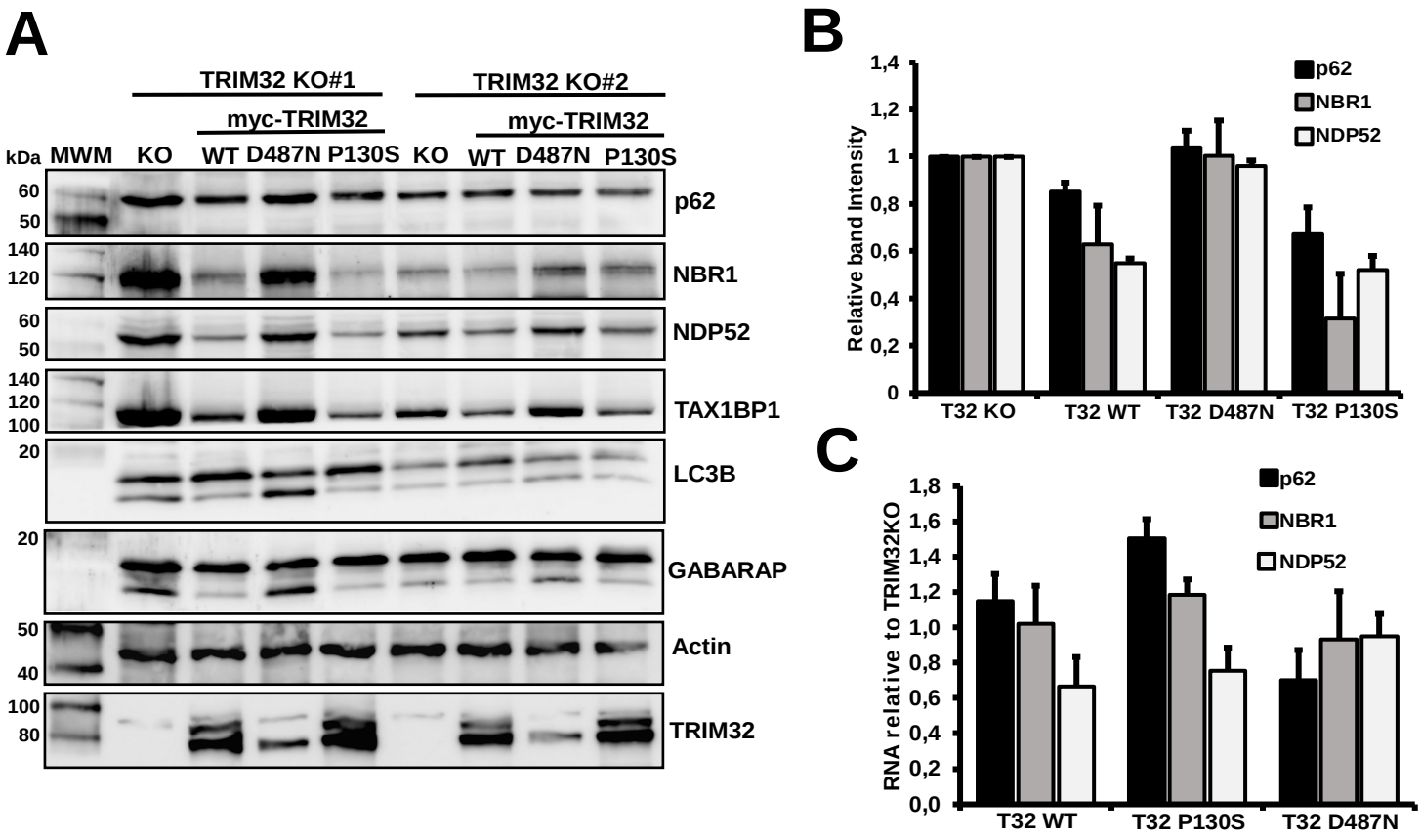
A
TRIM32 KO#1
TRIM32 KO#2
myc-TRIM32
myc-TRIM32
kDa MWM KO WT D487N P130S KO WT D487N P130S
60
50
p62
140
120
NBR1
60
50
NDP52
140
120
100
TAX1BP1
20
LC3B
20
GABARAP
50
40
Actin
100
80
TRIM32
B
Relative band Intensity
1,4
1,2
1
0,8
0,6
0,4
0,2
0
p62
NBR1
NDP52
T32 KO
T32 WT
T32 D487N
T32 P130S
C
RNA relative to TRIM32KO
1,8
1,6
1,4
1,2
1,0
0,8
0,6
0,4
0,2
0,0
p62
NBR1
NDP52
T32 WT
T32 P130S
T32 D487N

Figure 2

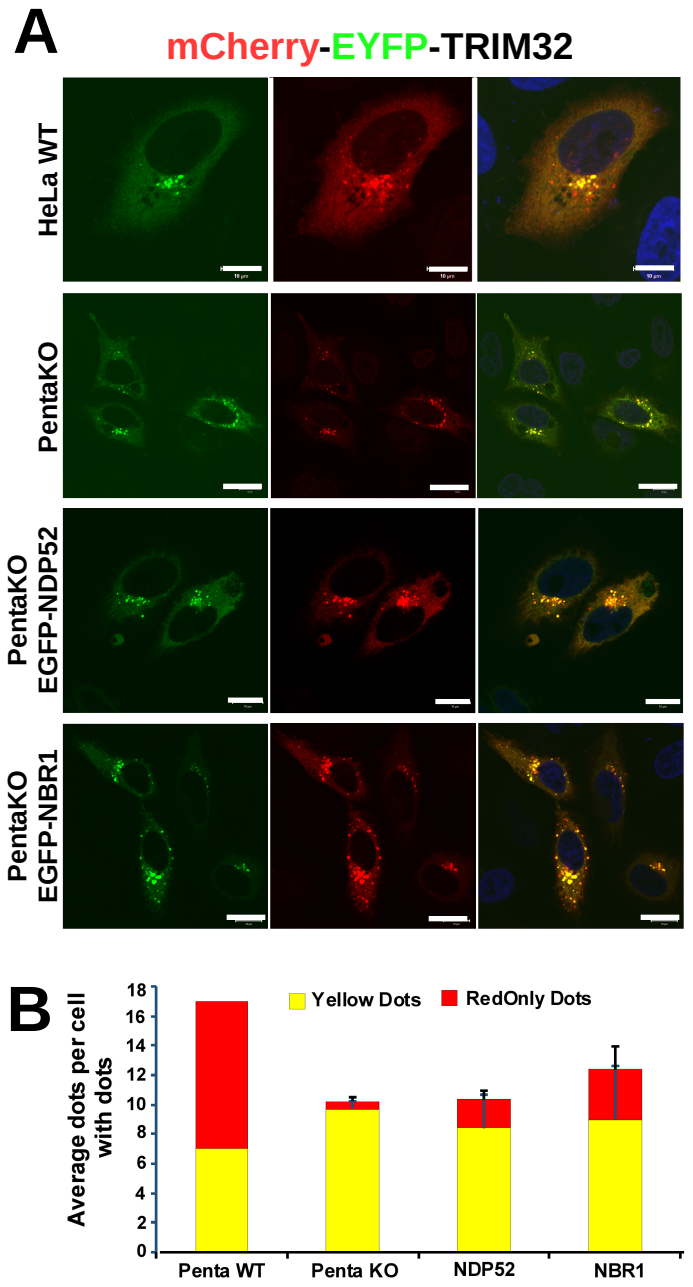
A
mCherry-EYFP-TRIM32
HeLa WT
PentaKO
PentaKO EGFP-NDP52
PentaKO EGFP-NBR1
B
Average dots per cell with dots
Yellow Dots
RedOnly Dots
0
2
4
6
8
10
12
14
16
18
Penta WT
Penta KO
NDP52
NBR1

Figure 3

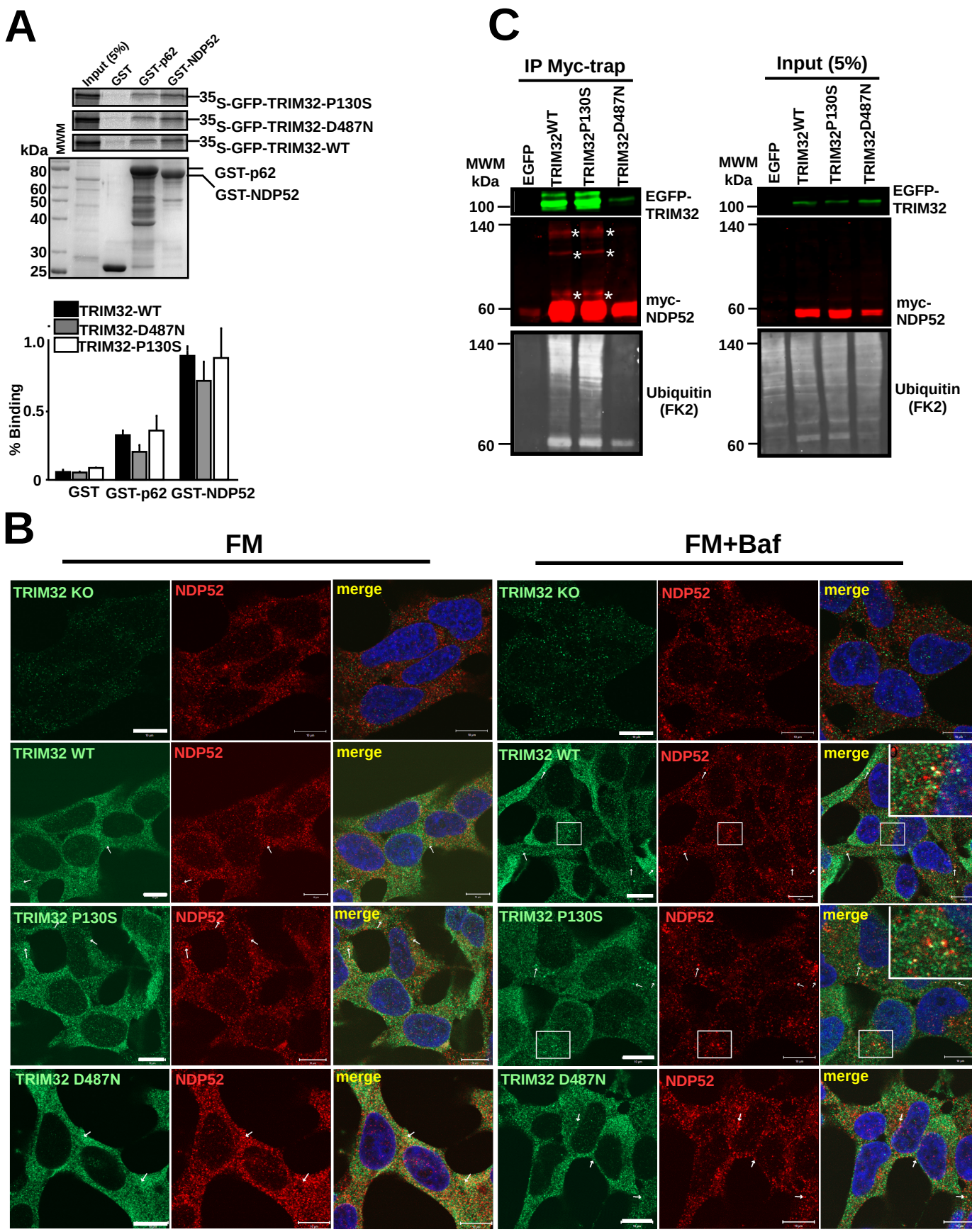
A
Input (5%)
GST
GST-p62
GST-NDP52
MWM
kDa
80
60
50
40
30
25
35S-GFP-TRIM32-P130S
35S-GFP-TRIM32-D487N
35S-GFP-TRIM32-WT
GST-p62
GST-NDP52
TRIM32-WT
TRIM32-D487N
TRIM32-P130S
% Binding
1.0
0.5
0
GST
GST-p62
GST-NDP52
C
IP Myc-trap
Input (5%)
MWM
kDa
EGFP
TRIM32WT
TRIM32P130S
TRIM32D487N
100
140
60
EGFP-
TRIM32
myc-
NDP52
Ubiquitin
(FK2)
B
FM
FM+Baf
TRIM32 KO
NDP52
merge
TRIM32 WT
TRIM32 P130S
TRIM32 D487N

Figure 4

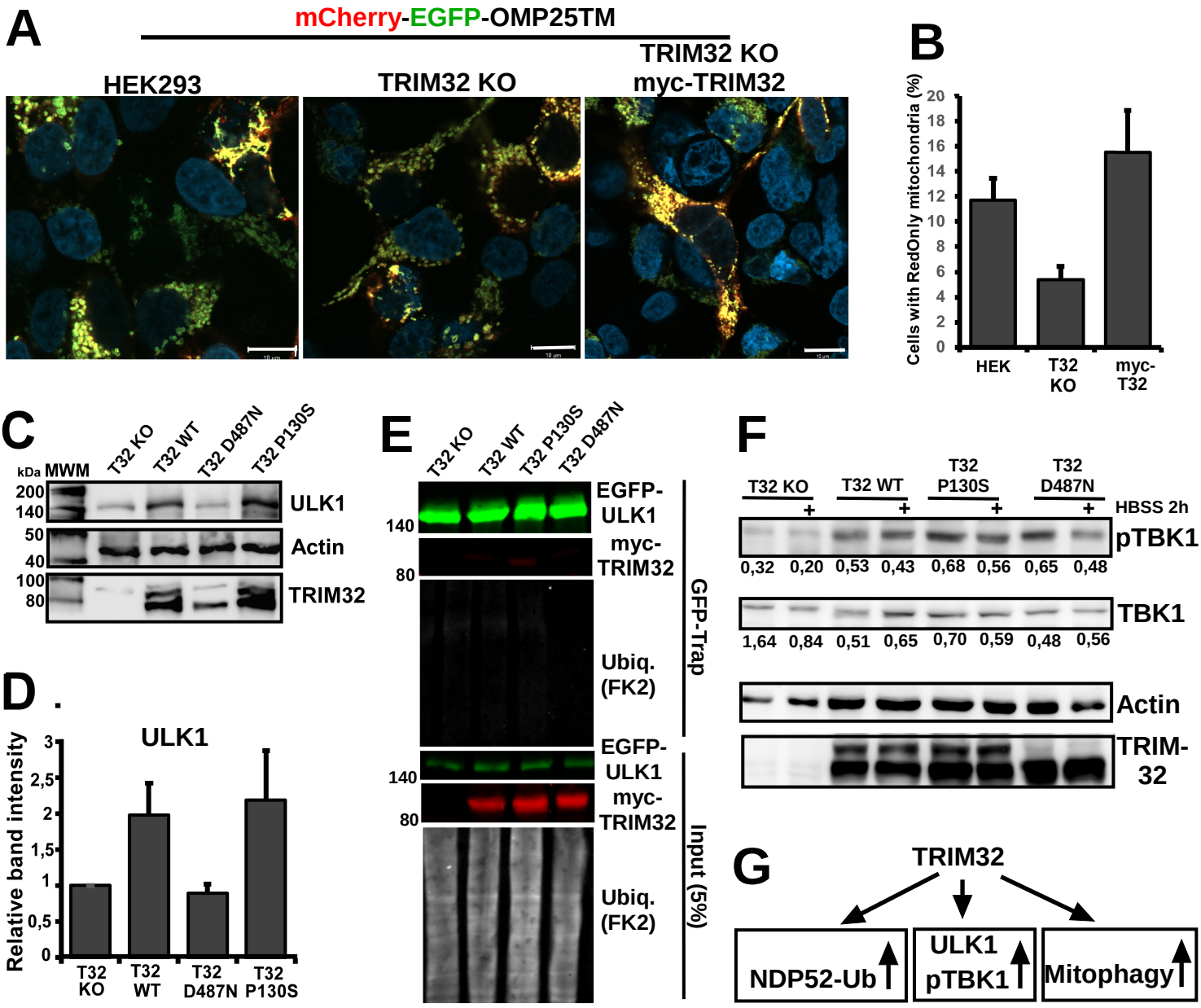
A
mCherry-EGFP-OMP25TM
HEK293
TRIM32 KO
TRIM32 KO
myc-TRIM32
B
Cells with RedOnly mitochondria (%)
0
2
4
6
8
10
12
14
16
18
20
HEK
T32 KO
myc-T32
C
kDa
MWM
T32 KO
T32 WT
T32 D487N
T32 P130S
200
140
50
40
100
80
ULK1
Actin
TRIM32
D
ULK1
Relative band intensity
0
0,5
1
1,5
2
2,5
3
T32 KO
T32 WT
T32 D487N
T32 P130S
E
T32 KO
T32 WT
T32 P130S
T32 D487N
140
80
EGFP-ULK1
myc-TRIM32
Ubiq. (FK2)
GFP-Trap
140
80
EGFP-ULK1
myc-TRIM32
Ubiq. (FK2)
Input (5%)
F
T32 KO
T32 WT
T32 P130S
T32 D487N
HBSS 2h
+
+
+
+
pTBK1
0,32 0,20 0,53 0,43 0,68 0,56 0,65 0,48
TBK1
1,64 0,84 0,51 0,65 0,70 0,59 0,48 0,56
Actin
TRIM-32
G
TRIM32
NDP52-Ub
ULK1
pTBK1
Mitophagy